Applied Ocean Research 33 (2011) 23–30

Contents lists available at ScienceDirect

Applied Ocean Research

journal homepage: www.elsevier.com/locate/apor

Evaluation of two WAM white capping parameterizations using parallel unstructured SWAN with application to the Northern Gulf of Mexico, USA

S. Mostafa Siadatmousavi [a,b,*], F. Jose [a], G.W. Stone [a,b]

[a] Department of Oceanography and Coastal Sciences, Louisiana State University, Baton Rouge, LA 70803, USA

[b] Coastal Studies Institute, Louisiana State University, Baton Rouge, LA 70803, USA

ARTICLE INFO

Article history:
Received 7 August 2010
Received in revised form
21 October 2010
Accepted 8 December 2010
Available online 30 December 2010

Keywords:
White capping
Parallel unstructured SWAN
WAM
Saturation spectrum
Gulf of Mexico

ABSTRACT

The performance of two well accepted formulations for white capping and wind input of third generation wave models, viz., WAM-3 and WAM-4, were investigated using parallel unstructured SWAN (PunSWAN). Several alternative formulations were also considered to evaluate the effects of higher order steepness and wave number terms in white capping formulations. Distinct model configurations were calibrated and validated against available *in situ* measurements from the Gulf of Mexico. The results showed that some of the *in situ* calibrated models outperform the saturation level calibrated models in reproducing the idealized wave growth curves. The simulation results also revealed that increasing the power of the steepness term can enhance the accuracy of significant wave height (H_s), at the expense of a higher bias for large waves. It also has negative effects on mean wave period (T_a) and peak wave period (T_p). It is also demonstrated that the use of the quadratic wave number term in the WAM-3 formulation, instead of the existing linear term, ameliorates the T_a underestimation; however, it results in the model being unable to reach any saturation level. In addition, unlike H_s and T_p, it has been shown that T_a is sensitive to the use of the higher order WAM-4 formulation, and the bias is decreased over a wide range of wave periods. However, it also increases the scatter index (SI) of simulated T_a. It is concluded that the use of the WAM-4 wind input formulation in conjunction with the WAM-3 dissipation form, is the most successful case in reproducing idealized wave growth curves while avoiding T_a underestimation of WAM-3 and a potential spurious bimodal spectrum of WAM-4; consequently, this designates another perspective to improve the overall performance of third generation wave models.

1. Introduction

Third generation wave models which solve the spectral form of the action balance equation [1] are efficient tools for simulating wave fields in medium- and large-scale domains [2]. Unlike earlier generations, these phase-averaged models include nonlinear wave–wave interaction, and dissipation terms without any prior assumption of spectral shape [3,4]. Among source/sink terms in deep water (wind input, quadruplet wave–wave interaction and energy dissipation [5]), dissipation is widely considered to be the least understood term [6]. Although several different formulations have been proposed for energy dissipation in deep water [6–10], the pulse-based quasi-linear model for the white capping term proposed by Hasselmann [11] remains in use in third generation wave models [12,13]. This approach successfully reproduces the fully developed wind–sea when used in conjunction with efficient quadruplet nonlinear wave interaction formulation referred to as the Discrete Interaction Approximation (DIA) [14], and rescaled wind input formulation of [15,16]. These sets of equations are used in the WAM cycle 3 model and are referred to as WAM-3 hereafter.

Advancements in understanding of wave growth in open water led to a theoretical description of the wind input term, which results in an acceptable level of agreement with *in situ* measurements [17]. The WAM cycle 4 model (WAM-4) employs wind–wave energy transfer parameterization based on quasi-laminar theory, and also considered quadratic dependence of dissipation on the wave number to provide more flexibility in the formulation for white capping dissipation [18]. This formulation also became part of many recent third generation wave models [12,13,19].

The third generation model, Simulating Wave Nearshore (SWAN) [12], has been well suited for both parameterizations, WAM-3 and WAM-4, and hence provides a tangible platform to compare and contrast their performance. Although originally developed for shallow water, SWAN incorporates all source and sink terms for generation and propagation of waves in deep and shallow water, and has been verified for several geographic settings and for different met-ocean conditions [2,8,20–25].

* Corresponding author at: Coastal Studies Institute, Louisiana State University, Baton Rouge, LA 70803, USA. Tel.: +1 225 578 4728; fax: +1 225 578 2520.
E-mail address: ssiada1@lsu.edu (S.M. Siadatmousavi).

0141-1187/$ – see front matter © 2010 Elsevier Ltd. All rights reserved.
doi:10.1016/j.apor.2010.12.002

The free coefficients of wave models, in this case SWAN, are conventionally set so that the model can reproduce saturation level spectra, among which the one suggested by Pierson–Moskowitz (PM) is probably the most popular [26,27]. However, Rogers et al. [8] stated that the wave models reach the saturation energy level too slowly. Moreover, it is not possible to calibrate the model for all possible wind speeds, because the PM spectrum scales with wind speed while the model formulations are scaled with friction velocity. Finally, tuning the model for unlimited time and fetch conditions may not be a realistic representation of wave growth in real-world situations. Therefore, in this study, the free parameters are determined by comparing the simulated significant wave height (H_s), peak wave period (T_p) and averaged wave period (T_a) with *in situ* observations.

Although a classical approach to adjust the model parameters is implemented in this study, in which the model is calibrated and verified using *in situ* measurements [28], as a reference, the performance of the calibrated model is compared with the same model tuned for the PM spectrum. In addition, Rogers et al. [8] showed that using a higher order wave number term in white capping formulation of WAM-3 enhances the model performance when compared with *in situ* observations. An in-depth analysis of this model performance along with similar modifications to WAM-4 are presented in this study. The same modifications are also applied to the steepness term in the white capping formulation of WAM-3 (see Section 2.2) which has been assumed to be constant without any clear scientific explanation. Therefore, the main objective of this study is to evaluate the effect of possible modifications in WAM-3 and WAM-4 white capping formulations when compared with known fetch-limited and fully developed wave data as well as long term *in situ* measurements.

2. Model description

2.1. Wind input

The wind input source term in SWAN can be described by a superposition of linear and exponential wave growth terms:

$$S_{\text{in}}(\sigma,\theta) = A + BE(\sigma,\theta) \tag{1}$$

in which E is energy density over relative frequency σ and propagation direction θ. The linear growth rate A, is based on the expression proposed by Cavaleri and Rizzoli [29] and is generally important during the early stages of wave growth. There are two different formulations for the coefficient B in the exponential wave growth term in WAM-3 and WAM-4. In WAM-3 the rescaled version of the experimental formulation of Snyder is employed [15,16] whereas in WAM-4, a set of equations presented by Janssen [17] is used. The latter formulation is based on the quasi-linear theory of wave generation, and the energy exchange from wind to wave is taken into account by interaction of atmospheric boundary layer and sea surface roughness length [30].

It is not surprising that all of the aforementioned formulations for wind input are a function of wind speed. The wind velocity components for this study were extracted from the North American Regional Re-analyzed (NARR) database from the National Center for Environmental Prediction (NCEP/NOAA) server. The NARR data grid 221 covers the entire continental US and the Gulf of Mexico with a horizontal resolution of approximately 32 km. More details regarding the wind data used in this study can be found in [31].

2.2. White capping

The White capping formulations implemented in SWAN for WAM-3 and WAM-4 are given as

$$S_{wc\_\text{WAM3}} \equiv -C_{ds}\left(\frac{\tilde{k}^2}{\tilde{s}_{\text{PM}}^2}E_{\text{tot}}\right)^n \left(\frac{k}{\tilde{k}}\right)^m \tilde{\sigma}E(\sigma,\theta) \tag{2a}$$

$$S_{wc\_\text{WAM4}} \equiv -C_{ds}\left[(1-\delta)+\delta\left(\frac{k}{\bar{\tilde{k}}}\right)^m\right]E_{\text{tot}}^2\tilde{k}^3k\tilde{\sigma}E(\sigma,\theta) \tag{2b}$$

in which $\tilde{k}$, $\tilde{\sigma}$ and E_{tot} denote the mean wave number, mean frequency and total energy respectively. Moreover, $\tilde{s}_{\text{PM}} = \sqrt{3.02\times10^{-3}}$ denotes steepness of the PM spectrum. The parameters $n = 2$ and $m = 1$ are fixed in the original model, and the main tuning coefficients are C_{ds} and δ which are conventionally determined to reproduce H_s; resulted from a fully developed PM spectrum. There are some recent studies that show WAM-3 can perform better in terms of the T_a estimation, when $m > 1$. However, it also leads to overestimation of H_s [8,10]. In this study, a similar investigation is made for WAM-4 to evaluate the effects on the simulated bulk wave parameters, by using higher order wave number terms in the white capping sink term. While having some fair support from measurements [32,33], the original $n = 2$ in Eq. (2a) was originally introduced by Komen [16] for a fully developed spectrum. Since the steepness of the spectrum would not change in such an asymptotic condition, choosing any different value for n was equivalent to redefining the coefficient C_{ds}. This is not the case for "young sea" in which the steepness of the wave field is evolving. Thus the effect of higher order dependence of the dissipation term on the steepness is also worthy of investigation. Our initial numerical efforts showed that using $n < 2$ could initiate numerical instabilities in shallow waters, that persist for long time periods; therefore only larger values of n were further pursued.

2.3. Other physical processes

Nonlinear quadruplet wave interaction plays an important role in controlling the shape and evolution of the wave spectrum [14]. Although the accurate physical description of nonlinear energy transfer is available [34,35], it is computationally intensive and cannot be used in operational models. The DIA formulation is the most common method for calculating nonlinear quadruplet wave interactions and is used in phase-averaged wave models such as SWAN, Mike21 and WAVEWATCH-III [12,13,19]. Although considered three orders of magnitude faster than best implementations of exact representation of nonlinear energy transfer, DIA is criticized to be inaccurate in reproducing the full wave spectrum [8,10]. Considering only a few possible configurations from the complete set of quadruplet interactions, results in unrealistic shape of the wave spectrum in the high frequency end of the wave spectrum, and also a broader spectrum near peak frequency [7,10,36,37]. Since our focus was on operational use of wave models, and it has been shown that DIA is capable of reproducing bulk wave parameters with sufficient accuracy [38], we used DIA for this study.

As the *in situ* measurements used in this study, to evaluate the performance of Parallel Unstructured SWAN (PunSWAN), are from deep to intermediate depths, the coastal wave transformation processes are not expected to significantly influence the bulk wave parameters. Therefore, the models with the least computational requirements are employed for parameterization of coastal processes: The nonlinear triad interaction is considered according to Eldeberky [39], bed friction according to Hasselmann et al. [40], and depth-induced wave breaking according to Battjes and Janssen [41].

2.4. Mesh file

The computational grid requires enough resolution to accommodate the complex bathymetry of shallow water for accurate coastal wave modeling [42]. In the recent versions, especially since 40.72, SWAN employs a Finite Volume scheme, and affords

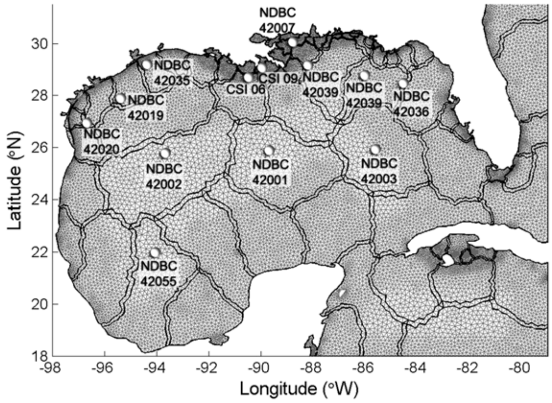

Fig. 1. Mesh file and its different partitions for parallel computing using 70 processors. The calculations for the common vertices along the boundaries are accomplished in both adjacent sub-grids. The locations of *in situ* met-ocean data monitoring in deep water (NDBC Buoys) and shallow water (WAVCIS CSI stations) used in this study, are also provided.

the use of the unstructured flexible mesh. In this study, the BatTri package [43] was used to generate the computational mesh file. Although the use of the implicit numerical scheme in SWAN ensures unconditional numerical stability, the accuracy of the result is highly dependent on mesh quality. Hence, additional precautions were taken during mesh generation to avoid a steep element slope, very small vertex angles, or even significant change in mesh size relative to the adjoining mesh elements [12]. The final mesh file is shown in Fig. 1, which consists of 32,235 nodes and 59,258 triangles with the element lateral length varying from 1 km nearshore to 50 km in deeper water. A higher mesh resolution is assigned where a sharp change in the wave spectrum is expected, such as shallow water. The unstructured flexible mesh approach affords us the opportunity to reduce the overall computational cost without compromising the accuracy along shallow waters.

In order to run PunSWAN, the mesh file was partitioned into sub-grids using *adcprep*, the grid preparation module of the circulation model ADCIRC [44]. The 70 mesh partitions are presented in Fig. 1. A linear speedup for PunSWAN was established on a Linux cluster with 35 nodes, each of them having two Intel(R) Xeon(TM) CPU 3.06 GHz processors and 2 GB RAM, which reaffirms the optimized parallelization of the SWAN source code [45].

3. Methods

3.1. Model calibration

As stated earlier, the conventional process of calibrating the model to be consistent with the PM spectrum, was critically revisited in recent literature [8,46]. Building on these studies, the tuning coefficients pertaining to white capping were determined by comparing the bulk wave parameters with *in situ* observations (see Fig. 1 for station locations). Wave, wind and meteorological data from the National Data Buoy Center (NDBC) and WAVCIS (Wave Current Surge Information System, www.wavcis.lsu.edu) [47] archives were used to evaluate the wind input data as well as wave model outputs. Since wave hindcasting is critically dependent on the accuracy of wind data [48,49], the quality of the input model wind used in the modeling were carefully analyzed. The NARR wind data for the period 15–31, March 2007 were shown to be very consistent with measured wind at all available stations [50] and used for the model calibration.

A total of 16 different configurations, as listed in Table 1, were used to evaluate the performance of WAM formulations in SWAN. For the WAM-3 formulation, the calibration was based on the bisection method on the parameter C_{ds} [51]. In order to compare the simulations, the H_s Scatter Index (SI) was calculated which is defined as follows [22,52]:

$$\mathrm{SI} \equiv \frac{\text{Root Mean Square Error of } H_s}{\text{Mean observed } H_s} = \frac{\sqrt{\frac{1}{N}\sum_{i=1}^{N}(H_{s,o}-H_{s,m})^2}}{\frac{1}{N}\sum_{i=1}^{N}H_{s,o}}. \quad (3)$$

In which $H_{s,o}$ and $H_{s,m}$ denote observed and measured H_s. The average of SI (ASI) from all stations was used as a measure of performance, and the calibration was terminated when ASI changed less than 0.1%. The WAM-4 formulation is a function of C_{ds} and δ. The parameter δ was changed from 0.1 to 0.9 (0.1 increment) and bisection method on the parameter C_{ds} was used to determine the minimal ASI. The optimal values of tuning parameters were determined for each case and are presented in Table 1.

3.2. Model verification during cold front season

The simulated bulk wave parameters during an active cold front season, from December 2007 to the end of April 2008 were compared with NDBC buoys and WAVCIS stations. Several cold front events as well as intermittent fair weather (calm) periods provided a realistic verification environment for the performance of SWAN using optimized tuning parameters already determined from the calibration process discussed above.

3.3. Model validation using idealized wave growth measurements

It is interesting to compare the performance of the wave model with generally accepted saturation spectra and asymptotic fetch-limited wave growth curves [7,8,10,46]. The idealized wave growth was performed with the structured 1D non-stationary formulation of SWAN. The reference depth was assigned as 3000 m to ensure deep water condition for all resulting wave fields. In addition, the wind speed was considered to be 15 m/s over the entire computational domain. This was the average wind speed in the database used to develop the PM spectrum. Moreover, the median fetch relevant to the PM (MFPM) database was approximately 350 km [53].

There are several available formulations based on asymptotic wave conditions. The growth curves of Young and Verhagen [54] suggest a set of equations that compares well with available data for both young and developed sea states, and are based on measurements from Lake George, Australia. That database was revisited by Breugem and Holthuijsen [55] and some outliers were removed due to coastline effects. The resulting growth curves are reduced to PM values for H_s for long fetches and those of Kahma and Calkoen [56] in fetch-limited condition. The JONSWAP experiment [40] also provides high quality fetch-limited wave growth database. The data were carefully studied by Kahma and Calkoen [56] and the highly variable wind data were removed to decrease the scatter of the dataset around the regression line. Kahma also provided another regression relationship for wave growth parameters in unstable conditions, based on Bothnian Sea measurements [57,58]. We took advantage of the revised formulations by Breugem and Holthuijsen [55], Kahma and Calkoen [56], and Kahma [57] as well as the saturation level data from the PM spectrum to evaluate the performance of different WAM formulations in the Gulf of Mexico.

4. Results and discussion

4.1. Calibration and verification

Quantitative calibration results of SWAN's performance, based on ASI for bulk wave parameters, are shown in Fig. 2. The cases

Table 1
List of model setups and the optimal values used for tuning white capping parameters C_{ds} and δ.

Parameter	Case name															
	W3-1	W3-2	W3-3	W3-4	W3-5	W3-6	W3-7	W3-8	W3-9	W4-1	W4-2	W4-3	W4-4	W4-5	W4-6	W-Mix
n	2	2	2	3	3	4	4	5	5	–	–	–	–	–	–	2
m	1	1	2	1	2	1	2	1	2	1	0.5	1	1.5	2	2.5	–
C_{ds}	2.36	1.2	1.14	0.76	1.06	0.46	0.99	0.28	0.85	4.5	2.0	1.75	1.5	1.0	0.75	2.02
δ	–	–	–	–	–	–	–	–	–	0.5	1.0	0.8	0.8	0.8	0.7	0.0

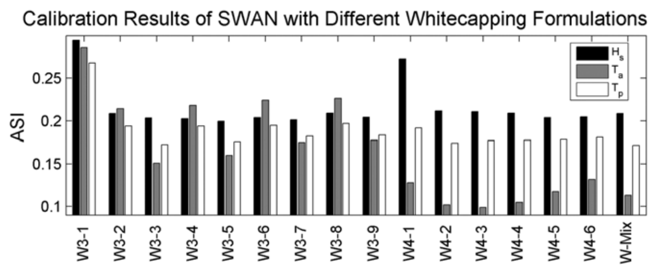

Fig. 2. Calibration result of SWAN using white capping parameterizations provided in Table 1.

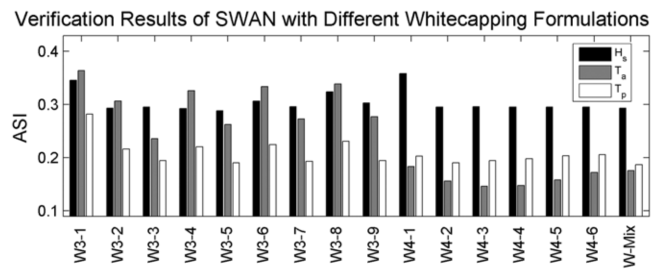

Fig. 3. Verification result of SWAN using white capping parameterizations provided in Table 1.

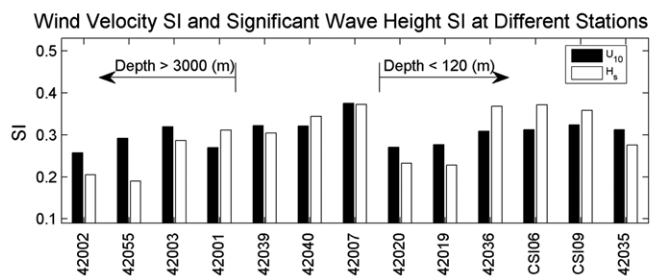

Fig. 4. Scatter Indices of wind speed and significant wave height (based on case W4-3) at different stations in Gulf of Mexico during the verification period. The stations are ordered from left to right based on depth.

W3-1 and W4-1 composed of the conventional default values suggested for WAM-3 and WAM-4 formulations respectively, based on the ability of the model to reproduce the PM spectrum [5]. The rationale in implementing all other model optimization simulations was to reproduce the *in situ* H_s with minimum ASI. Although all optimized H_s values are close, W3-2 and W3-5 cases resulted in slightly better agreement with measurements. The WAM-4 formulation performed significantly better in terms of T_a which is consistent with previously reported underestimation of T_a using WAM-3 [59]. Using the quadratic wave number term instead of the linear form in the WAM-3 formulation, also suggested by Rogers [8], addressed this problem considerably (e.g. comparison of W3-2 and W3-3). This is not surprising, because the higher order wave number terms in white capping formulation dissipates more energy in higher frequencies, resulting in lower mean frequency, or equivalently, higher T_a. The changes in $\tilde{k}$ and $\tilde{\sigma}$ further enhance this dissipation process.

Increasing the power of the steepness term in WAM-3 had negative impacts on bulk wave parameters when $n > 3$ was used. A slight improvement in H_s was attained, using $n = 3$ in Eq. (2a) in conjunction with either a linear or second order wave number term in the white capping sink term; however, it also resulted in poorer results for T_a and T_p. Using higher order wave number terms in WAM-4, white capping formulation also yielded slightly better H_s estimations (best result was found for W4-5), however, leading to poorer results pertaining to T_a. Finally, the case W-Mix showed the best T_p estimation, and also better T_a estimation than all WAM-3 cases.

The performance of the model using different formulations with well tuned calibration, were verified using an independent time period that lasted for five months. The verification results illustrated in Fig. 3 confirm that Eq. (2a) yields more realistic simulated T_a using the second order wave number term. It also validates the earlier conclusions regarding better performance of WAM-4 formulation in simulating T_a, and slightly better performance of W3-4 and W3-5 in simulating H_s. Similar to calibration results, case W4-5 yields better H_s prediction among WAM-4 formulations, and the W3-5 case shows the best H_s prediction among all cases. The better performance of case W-Mix than all WAM-3 runs, in terms of T_a, shows that a significant portion of underestimation in wave period underscores inferior performance of the wind input formulation used in WAM-3 when compared with that used in WAM-4. Again, the case W-Mix also demonstrates the best T_p estimation.

The SI of wind speed at 10 m above the surface (U10) at all *in situ* stations and SI of H_s resulted from case W4-3 is plotted in Fig. 4. The stations are ordered based on their depth. A slightly higher SI factor is obtained at shallow stations than at deep water stations; however, even at stations with water depth deeper than 120 m, which satisfy the deep water condition for $T_p < 12$ s, SI is high. Therefore the ASI of H_s shown in Fig. 3 is not a critical function of the depth of stations used in this study; and, therefore, shallow water wave processes have minor effects on the model accuracy; this appears to be mainly controlled by wind accuracy.

It is also worth to note that SWAN using the WAM-4 formulation, is approximately 30% more computationally expensive than the WAM-3 formulation. If the total time needed to perform nonlinear interaction is considered as reference time t_{nl}, the white capping dissipation term requires slightly more than $0.3t_{nl}$ using the WAM-3 or WAM-4 formulation. However, the wind input term in WAM-3 requires of the order of $0.2t_{nl}$ whereas WAM-4, which is 10 times more computationally intensive, requires approximately $2.3t_{nl}$.

4.2. *The effect of wave steepness on simulated wave conditions/higher order wave number*

The effects of increasing the power of wave steepness as a function of bias of bulk wave parameters are depicted in Fig. 5, for several representative WAM-3 alternatives. Panel (A) shows that case W3-2 (default value for steepness power) works well for wave heights larger than 1.4 m. However, case W3-4 predictions are slightly better for H_s smaller than 1.4 m which constitutes 68% of wave records used in the analysis. Therefore, over the entire wave

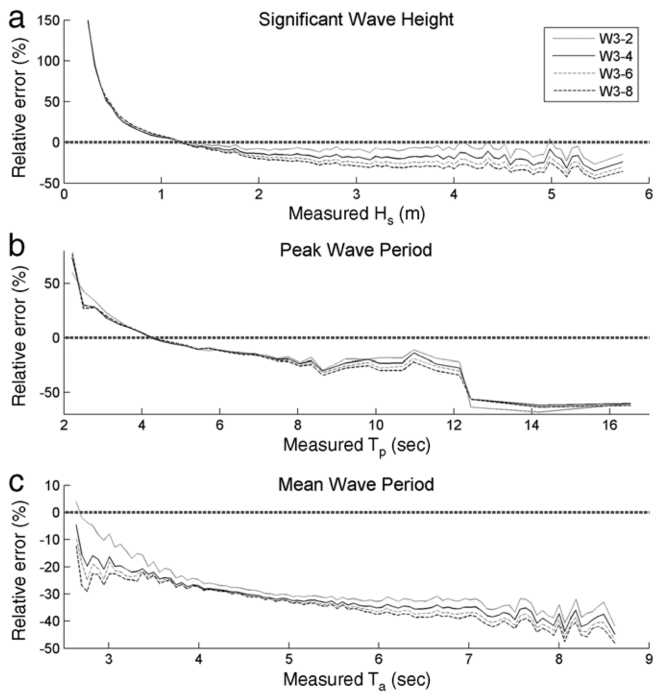

Fig. 5. The effect of increasing steepness power in white capping equation of WAM-3 on the simulation of bulk wave parameters. Note that the bias of scatter data were averaged over 0.05 m intervals for H_s, 0.3 s for T_p and 0.05 s for T_a, to remove fluctuations and keep the trend.

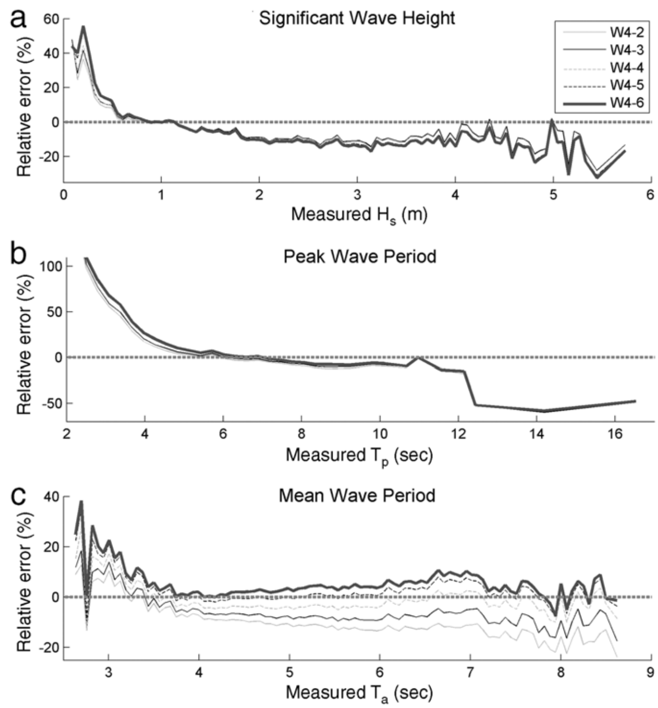

Fig. 6. The effect of increasing wave number power in white capping equation of WAM-4 on the simulation of bulk wave parameters. Note that the bias of scatter data were averaged over 0.05 m intervals for H_s, 0.3 s for T_p and 0.05 s for T_a, to remove fluctuations and keep the trend.

record from all stations shown in Fig. 1, case W3-4 outperforms the other cases. Panel (B) shows that case W3-2 performs better over a larger portion of the wave period range. As shown in Panel (C), W3-2 also shows a significantly smaller bias for T_a than all other cases. Therefore, increasing the coefficient n in Eq. (2a) consistently increases the bias in bulk wave parameters.

The effects of increasing the power of the wave number term in the white capping formulation of WAM-4, based on the bias of simulated bulk wave parameters, are presented in Fig. 6. Panels (A) and (B) show that the modification has minor effects on the model performance in terms of H_s and T_p. The default value $m = 1$ (case W4-3) works well for H_s larger than 1 m; however for smaller wave heights, case W4-2 leads to better model performance. Panel (B) shows that T_p is only affected for $T_p < 5$ s and decreasing the coefficient m in Eq. (2b) results in slightly less bias. Although case W4-2 surpasses all other cases in T_p performance, case W4-5 has much less bias for T_a from 3.5 to 6 s which constitutes 87% of the wave record. It also performs well for longer wave periods; while for smaller periods, W4-2 results in the minimum bias. Increasing the coefficient m in Eq. (2b) can ameliorate T_a underestimation for wave periods larger than 3.5 s although decreasing the coefficient m can enhance the model results for smaller wave periods. Also, it is noteworthy that the large relative errors in both Figs. 5 and 6 for $T_p > 13$ s were resulted from a limited number of samples (this occurred only 6 times at all stations altogether) and can be explained in terms of significant overestimation of energy measured by buoys at the low end of the spectrum during calm conditions; as was reported recently by Work [60].

4.3. Idealized wave growth

The simulated non-dimensional energy and peak wave frequency using WAM-3 and WAM-4 formulations are skill assessed with different *in situ* idealized wave growth datasets, as shown in Figs. 7 and 8. It is apparent that all parameterizations overestimate the energy level for short fetches; and the overestimation is generally more intense using WAM-3 than WAM-4 alternatives. Moreover, all cases overestimate the peak frequency at MFPM. Comparison between the default WAM-3 (case W3-1) and default WAM-4 (case W4-1) parameterizations for wind input and white capping terms show that default WAM-3 parameterization reaches its saturation level at the fetch which is closer to MFPM; however, the energy level is lower than PM. The saturated energy level and also peak frequency, are very close to PM values when using WAM-4, although at a fetch which is one order of magnitude larger than MFPM.

The models calibrated using *in situ* measurements show better agreement with the PM energy level and peak frequency, while, similar to W3-1 and W4-1, require longer fetch than MFPM to reach the saturation energy levels. Except for W4-5, the rest of WAM-4 formulations and also the W-Mix case, perform better than WAM-3 formulations in limited fetches. All cases except W3-3, W3-5 and W4-5, lead to good agreement with peak frequency in short fetches; and WAM-3 alternatives (excluding W3-3 and W3-5) result in higher peak wave frequency than WAM-4 alternatives in long fetches.

Comparing cases W3-2 and W3-4 reveals that increasing the power of the steepness term can improve WAM-3 results in short fetches significantly. The energy level computed for long fetches is also in better agreement with the PM value; however, a longer fetch is needed to reach the PM energy level. It is also interesting to note that the case W-Mix outperforms all *in situ* calibrated cases in short fetches, and the energy level at MFPM is close to PM. The saturation energy level for W-Mix is also close to that of the PM spectrum. This again confirms that wind input parameterization plays an important role on model performance, and part of WAM-3's poor to average performance may be a consequence of oversimplifications in the wind input term.

Significant overestimation associated with short fetches and high energy gradients over the entire fetch ranges, for the cases

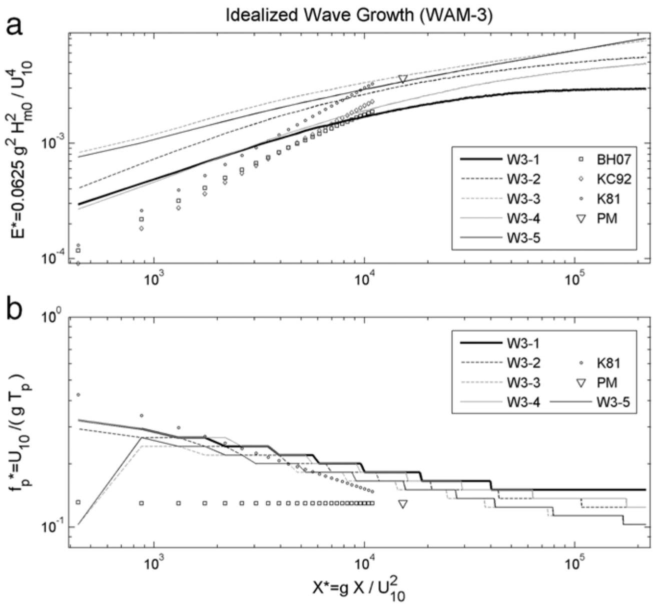

Fig. 7. Deep water fetch-limited growth curve produced from WAM-3 alternatives and *in situ* measurements of Breugem and Holthuijsen [55] (BR07), Kahma and Calkoen [56] (KC92), Kahma [57] (K81) and Pierson and Moskowitz [26] (PM). The constant wind speed, $U_{10} = 15$ m/s is used in all cases. The fetch value of $X = 350$ km is used for PM value which is the median of the database used to produce PM spectrum. Note that the first moment of wave spectrum, H_{m0}, is used to calculate non-dimensional energy which is close to H_s is deep water.

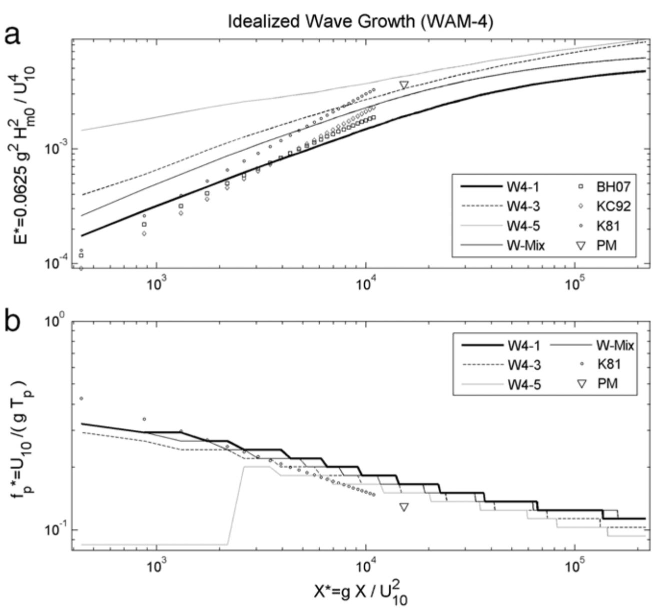

Fig. 8. Deep water fetch-limited growth curve produced from WAM-4 alternatives and *in situ* measurements of Breugem and Holthuijsen [55] (BR07), Kahma and Calkoen [56] (KC92), Kahma [57](K81) and Pierson and Moskowitz [26] (PM). The constant wind speed, $U_{10} = 15$ m/s is used in all cases.

with higher order wave number terms (cases W3-3, W3-5, W4-5), reveal the inability of these models to reach a saturation level. In addition, these models show peculiarly low peak frequency for short fetch scenarios. The spectrum evolution (e.g. Fig. 9) explains the reason for both of these abnormal behaviors. The nonlinear wave interaction redistributes energy from peak frequency towards lower and higher frequencies. Increasing the power of the white capping term in Eqs. (2a) and (2b) results in less dissipation in low frequencies, and part of this transferred energy may have been retained with time. The accumulation of the

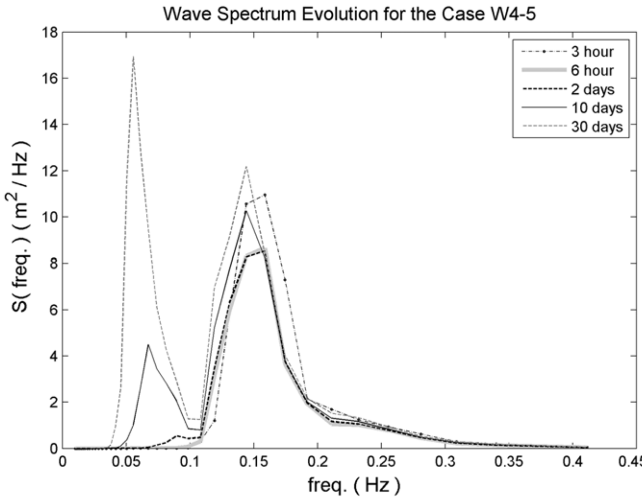

Fig. 9. The evolution of wave spectrum at $X = 35$ km ($X^* \approx 1526$) for the case W4-5.

residual energy generates an unrealistic bimodal wave spectrum for wind–sea conditions if the energy transfer from DIA continues (e.g. during steady wind conditions). Since the white capping dissipation is small in low frequencies, there is no mechanism to dissipate the energy of low frequency peak; therefore it continues to grow slowly, and eventually becomes the dominant peak in the wave spectrum as shown in Fig. 7 for W3-3 and W3-5, and in Fig. 8 for W4-5.

The time needed for each case to attain the wave growth independent of wind duration, and for a fixed fetch of 350 km ($X =$ MFPM), is presented in Table 2. The values were determined by seeking the first time step for which both H_s and T_p exceed 95% of their final values (after 30 days). The Moskowitz [53] database used for the PM spectrum shows that the median time equals 12 h; However, unlike the simulation, the initial conditions were not calm. Hence, all cases except for W3-3, W3-5, and W4-5 are considered to be in good agreement with the Moskowitz measurements. The long durations determined for cases W3-3, W3-5, and W4-5 reaffirm that the energy accumulation at low frequencies deprives the model from reaching any equilibrium stage.

5. Summary and conclusions

Based on the work presented above, the following summary and conclusions are presented.

Parallel unstructured mesh implementation of the third generation wave model, SWAN, was used to compare the performance of the most common formulations of white capping and wind input, WAM-3 and WAM-4. Traditionally the model parameters were calibrated using bulk wave parameters of fully developed conditions such as the PM spectrum; however, in order to avoid the recent criticism associated with this approach, in this study the model was first calibrated and validated using *in situ* H_s measurements from NDBC buoys and WAVCIS stations from the Gulf of Mexico. This process significantly enhanced the performance of SWAN in the simulation of bulk wave parameters for the Northern Gulf of Mexico.

The calibration process was repeated for several alternatives of WAM-3 and WAM-4 with higher order steepness and wave number terms. Although all configurations resulted in a similar level of accuracy for H_s, the performance of SWAN with each configuration was different in simulating wave period and reproducing idealized wave growth spectra.

Table 2
Time needed for different cases at the fetch equal to MFPM to reach duration-unlimited saturation condition.

Case	W3-1	W3-2	W3-3	W3-4	W3-5	W4-1	W4-3	W4-5	W-Mix
Time (h)	15	14	139	15	305	17	174	375	15

Increasing the power of the steepness term in the WAM-3 formulation from 2 to 3 (case W3-4) slightly decreased the ASI of H_s and also improved the resulting bias for small H_s and short T_p; however, this was not apparent for H_s larger than 1.4 m. Over the entire wave record, the bias effect was negligible for H_s and T_p; although not the case for T_a hindcasting. Lower values for the power of the steepness term than the default $n = 2$ in the WAM-3 formulation resulted in numerical problems in shallow water, implying that n should be kept in the range 2–3. Surprisingly, the use of $n = 3$ and parameters determined from *in situ* calibration outperforms the original PM calibrated WAM-3 case in reproducing fetch-limited growth curves as well as the PM saturation level for the wave spectrum.

The results show that all WAM-3 alternatives underestimate T_a. Increasing the wave number power from 1 to 2 can considerably address this problem by direct dissipation of energy in the high frequency end of the wave spectrum, and indirect effects of changing the mean wave number and wave frequency. However, the model is unable to maintain any saturation level, and the spurious energy transfer to the low frequency portion of the wave spectrum could result in a bimodal wave spectrum for steady wind–sea conditions. It is concluded that case W3-3 is more successful than all other cases in the Gulf of Mexico; however, it is not suitable for steady wind conditions; and case W3-4 is recommended for such weather conditions.

The use of $m = 2$ instead of 1 in white capping formulation of WAM-4 has negligible effects on H_s and T_p. It also enhances the bias of T_a when $T_a > 3.5$ s; however, it slightly increases the ASI. Incorporation of higher order wave number terms in WAM-4 also results in the model being prone to developing a bimodal energy spectrum and unlimited wave growth in unlimited fetch and time duration conditions. Therefore case W4-3 is the recommended model parameter in the WAM-4 formulation in the Gulf of Mexico.

Although WAM-4 wind input is 10 times more computationally expensive than WAM-3 wind input formulation and results in approximately a 30% extension in total computational time, it enhances the overall performance of the model. The use of WAM-4 wind input formulation in conjunction with WAM-3 white capping formulation was the most successful combination in hindcasting T_p. It also outperforms all WAM-3 alternatives in the estimation of T_a, while avoiding the potential spurious bimodal spectrum observed using *in situ* calibration of the WAM-4 dissipation term. Indications are evident that the wind input formulation also plays an important role in the performance of wave models, and part of their below par performance can be resolved by modifying the wind input term instead of the white capping term.

Acknowledgements

The authors wish to thank Dr. Marcel Zijlema for sharing the source code of PunSWAN. Jonathan R. Shewchuk (UC-Berkeley) is also gratefully acknowledged for providing the Triangle grid generation tool. We acknowledge the Coastal Studies Field Support Group, and chief engineer Bill Gibson for WAVCIS operations.

References

[1] Whitham GB. A general approach to linear and non-linear dispersive waves using a Lagrangian. J Fluid Mech 1965;22:273–83.
[2] Zubier K, Panchang V, Demirbilek Z. Simulation of waves at duck (North Carolina) using two numerical models. Coast Eng J 2003;45:439–69.
[3] WAMDI Group. The WAM model—a third generation ocean wave prediction model. J Phys Oceanogr 1988;18.
[4] Massel SR. Ocean surface waves: their physics and prediction. World Scientific; 1996.
[5] Komen GJ, Cavaleri L, Donelan M, Hasselmann K, Hasselmann S, Janssen PAEM. Dynamics and modelling of ocean waves. Cambridge: Cambridge University Press; 1994.
[6] Cavaleri L, Alves J-HGM, Ardhuin F, Babanin A, Banner M, Belibassakis K, et al. Wave modelling: the state of the art. Prog Oceanogr 2007;75:603–74.
[7] Tolman HL, Chalikov D. Source terms in a third-generation wind wave model. J Phys Oceanogr 1996;26:2497–518.
[8] Rogers WE, Hwang PA, Wang DW. Investigation of wave growth and decay in the SWAN model: three regional-scale applications. J Phys Oceanogr 2003;33:366–89.
[9] Babanin AV, Tsagareli KN, Young IR, Walker DJ. Numerical investigation of spectral evolution of wind waves. Part II: dissipation term and evolution tests. J Phys Oceanogr 2010;40:667–83.
[10] van der Westhuysen AJ, Zijlema M, Battjes JA. Nonlinear saturation-based whitecapping dissipation in SWAN for deep and shallow water. Coast Eng 2007;54:151–70.
[11] Hasselmann K. On the spectral dissipation of ocean waves due to whitecapping. Bound-Layer Meteorol 1974;6:107–27.
[12] SWAN team. SWAN cycle III version 40.81. Scientific and technical documentation. 2010. p. 126.
[13] Tolman HL. User manual and system documentation of WAVEWATCH III TM version 3.14. 2009. p. 220.
[14] Hasselmann S, Hasselmann K, Allender JH, Barnett TP. Computations and parameterizations of the nonlinear energy-transfer in a gravity-wave spectrum. 2. Parameterizations of the nonlinear energy-transfer for application in wave models. J Phys Oceanogr 1985;15:1378–91.
[15] Snyder RL, Dobson FW, Elliott JA, Long RB. Array measurements of atmospheric-pressure fluctuations above surface gravity-waves. J Fluid Mech 1981;102:1–59.
[16] Komen GJ, Hasselmann S, Hasselmann K. On the existence of a fully-developed wind–sea spectrum. J Phys Oceanogr 1984;14:1271–85.
[17] Janssen PAEM. Quasi-linear theory of wind-wave generation applied to wave forecasting. J Phys Oceanogr 1991;21:1631–42.
[18] Janssen PAEM. The interaction of ocean waves and wind. Cambridge University Press; 2004.
[19] Sorensen OR, Kofoed-Hansen H, Rugbjerg M, Sorensen LS. A third-generation spectral wave model using an unstructured finite volume technique. In: International conference on coastal engineering 292004. p. 894–906.
[20] Rogers WE, Kaihatu JM, Hsu L, Jensen RE, Dykes JD, Holland KT. Forecasting and hindcasting waves with the SWAN model in the Southern California bight. Coast Eng 2007;54:1–15.
[21] Zijlema M, van der Westhuysen AJ. On convergence behaviour and numerical accuracy in stationary SWAN simulations of nearshore wind wave spectra. Coast Eng 2005;52:237–56.
[22] Moeini MH, Etemad-Shahidi A. Application of two numerical models for wave hindcasting in Lake Erie. Appl Ocean Res 2007;29:137–45.
[23] Kagan BA, Alvarez O, Gorchakov EV. Weak dependence of the SWAN wave model on hydrodynamic properties of sea bottom. Izv Atmos Ocean Phys 2008;44:781–6.
[24] Palmsten ML. Application of SWAN wave model to a high-energy continental shelf: University of South Florida; 2001.
[25] Zhang D, Kiu H, Lin P. The application of SWAN to the simulation of a storm surge. In: International conferene on estuaries and coasts. 2003.
[26] Pierson WJ, Moskowitz L. Proposed spectral form for fully developed wind seas based on similarity theory of *s* a Kitaigorodskii. J Geophys Res 1964;69:5181–90.
[27] Massel SR. Ocean waves breaking and marine aerosol fluxes. New York: Springer; 2007.
[28] Kamphuis JW. Introduction to coastal engineering and management. 2000. p. 472.
[29] Cavaleri L, Rizzoli PM. Wind wave prediction in shallow-water—theory and applications. J Geophys Res-Oc Atm 1981;86:961–73.
[30] Janssen PAEM. Wave-induced stress and the drag of air-flow over sea waves. J Phys Oceanogr 1989;19:745–54.
[31] Siadatmousavi SM, Jose F, Stone GW. Simulating hurricane Gustav and Ike wave fields along the Louisiana innershelf: implementation of an unstructured third-generation wave model. SWAN. In: Proc. Oceans'09. 2009.
[32] Kraan C, Oost WA, Janssen PAEM. Wave energy dissipation by whitecaps. J Atmos Ocean Tech 1996;13:262–7.
[33] Lafon C, Piazzola J, Forget P, Le Calve O, Despiau S. Analysis of the variations of the whitecap fraction as measured in a coastal zone. Bound-Layer Meteorol 2004;111:339–60.

[34] Zakharov VE. Stability of periodic waves of finite amplitude on the surface of a deep fluid. J Appl Mech Tech Phys 1968;9:190–4.
[35] Hasselmann K. On the non-linear energy transfer in a gravity-wave spectrum part 1. General theory. J Fluid Mech 1962;12:481–500.
[36] Van Vledder G, Bottema M. Improved modelling of nonlinear four-wave interactions in shallow water. In: 28th international conference on coastal engineering. ASCE. 2003. p. 459–71.
[37] van Vledder GP. The WRT method for the computation of non-linear four-wave interactions in discrete spectral wave models. Coast Eng 2006;53: 223–242.
[38] Janssen PAEM, Günther H, Hasselmann S, Hasselmann K, Komen GJ, Zamberesky L. Simple tests. In: Komen GJ, Cavaleri L, Donelan M, Hasselmann K, Hasselmann S, Janssen PAEM, editors. Dynamics and modelling of ocean waves. Cambridge University Press; 1994. p. 556.
[39] Eldeberky Y. Nonlinear transformations of wave spectra in the nearshore zone. The Netherlands: Delft University of Technology; 1996.
[40] Hasselmann K, Barnett TP, Bouws E, Carlson H, Cartwright DE, Enke K, et al. Measurements of wind-wave growth and swell decay during the joint north sea wave project (JONSWAP). Deutsche Hydrogr Z 1973;8(12):95.
[41] Battjes JA, Janssen JPFM. Energy loss and set-up due to breaking of random waves. In: 16th international conference on coastal engineering. ASCE. 1978. p. 569–87.
[42] Hagen SC, Horstman O, Bennett RJ. An unstructured mesh generation algorithm for shallow water modeling. Int J Comput Fluid Dyn 2002;16:83–91.
[43] Bilgili A, Smith KW, Lynch DR. BatTri: a two-dimensional bathymetry-based unstructured triangular grid generator for finite element circulation modeling. Comput Geosci (UK) 2006;32:632–42.
[44] Westerink JJ, Luettich RA, Baptista AM, Scheffner NW, Farrar P. Tide and storm-surge predictions using finite-element model. J Hydraul Eng, ASCE 1992;118: 1373–90.
[45] Zijlema M. Multiscale simulations using unstructured mesh SWAN model for wave hindcasting in the Dutch Wadden Sea. Tokyo (Japan): Coastal dynamics 09; 2009. p. 1–12.
[46] Booij N, Ris RC, Holthuijsen LH. A third-generation wave model for coastal regions, 1. Model description and validation. J Geophys Res 1999;104: 7649–66.
[47] Stone GW, Zhang XP, Gibson W, Frederichs R. A new wave-current online information system for oil spill contigency planning (WAVCIS). In: 24th arctic and marine oil spill program technical seminar. 2001. p. 401–25.
[48] Sarkar RKA, Aggarwal VK, Bhatt V, Bhaskaran PK, Dube SK. Ocean wave model-sensitivity experiments. In: International conference PORSEC-2000 NIO. 2000. p. 621–7.
[49] Janssen PAEM. Progress in ocean wave forecasting. J Comput Phys 2008;227: 3572–94.
[50] Siadatmousavi SM, Jose F, Stone GW. The effects of bed friction on wave simulation: implementation of an unstructured third-generation wave model. SWAN. J Coast Res 2010 [under reveiw].
[51] Burden RL, Faires JD. Numerical analysis. 7th ed. Pacific Grove (CA): Brooks Cole; 2001.
[52] Lin WQ, Sanford LP, Suttles SE. Wave measurement and modeling in Chesapeake Bay. Cont Shelf Res 2002;22:2673–86.
[53] Moskowitz L. Estimates of power spectrums for fully developed seas for wind speeds of 20 to 40 knots. J Geophys Res 1964;69:5161–79.
[54] Young IR, Verhagen LA. The growth of fetch limited waves in water of finite depth. 1. Total energy and peak frequency. Coast Eng 1996;29:47–78.
[55] Breugem WA, Holthuijsen LH. Generalized shallow water wave growth from Lake George. J Waterw Port C, ASCE 2007;133:173–82.
[56] Kahma KK, Calkoen CJ. Reconciling discrepancies in the observed growth of wind-generated waves. J Phys Oceanogr 1992;22:1389–405.
[57] Kahma KK. A study of the growth of the wave spectrum with fetch. J Phys Oceanogr 1981;11:1503–15.
[58] Young IR. Wind generated ocwan waves. Elsevier; 1999.
[59] Ris RC, Holthuijsen LH, Booij N. A third-generation wave model for coastal regions—2. Verification. J Geophys Res Oceans 1999;104:7667–81.
[60] Work PA. Nearshore directional wave measurements by surface-following buoy and acoustic Doppler current profiler. Ocean Eng 2008;35:727–37.